DOI: 10.1021/ic902538a

Inorganic Chemistry
Article

Color Tuning of Direct White Light of Lanthanum Aluminate with Mixed-Valence Europium

Zhi-yong Mao[†,‡] and Da-jian Wang[*,‡,§]

[†]*School of Materials Science and Engineering, Tianjin University of Technology, Tianjin 300384, People's Republic of China,* [‡]*Key Laboratory of Display Materials and Photoelectric Devices, Tianjin University of Technology, Ministry of Education, Tianjin 300384, People's Republic of China, and* [§]*Tianjin Key Laboratory of Photoelectronic Materials and Devices, Tianjin 300384, People's Republic of China*

Received December 20, 2009

The generation of direct white-light emission of the coexisting valence-varied europium−lanthanum aluminate through substitution of cations into the host and its resultant adjustment of the energy transfer have been presented. With respect to $La_{0.99-x}Sr_xAlO_{3-\delta}$:$Eu_{0.01}$ and $La_{0.994}Al_{1-x}O_{3-\delta}$:$Eu_{0.006}$, and Mn_x, $Li_{0.012}$, the green-light emission positioned at 515 nm plays a key role to color mix for white light and can be efficiently tuned by adjusting the transfer of energy and relevant transition emissions between the luminous centers of Eu^{2+} and Eu^{3+}/Mn^{2+}, via varying amounts of dopants. Direct white-light emission with optimized values of 86 for the color rendering index and 5091 K for the correlated color temperature has been achieved for lanthanum aluminate by this mixed-valence means.

Introduction

New inorganic phosphor materials applied in lighting and display fields have being extensively developed, particularly those used for white-light-emitting devices with the recent progress of semiconductor luminescence technology.[1−6] Also, phosphors of single-host full-color emission, rather than a commonly used multicomponent phosphor mixture, pumped with ultraviolet (UV)/blue light to produce white light directly have attracted great attention, driven by their advantages to overcome the drawbacks of self-absorption and complex blending operations, usually leading to a decrease of the device efficiency. Direct white-light strategies with a designed quality of white light have drawn much interest recently, ranging from semiconducting nanocrystals,[7−9] organic compounds,[10−12] complexes,[13,14] microporous materials,[15] and inorganic−organic hybrid hosts[16] to rare-earth-doped inorganic phosphors.[17−20] Alternatively, abnormal mixed valences of Eu ions in some specific inorganic compounds have been widely observed,[21−23] resulting from their substantial structural chemistry; consequently, the optimal combination of an individual spectrum for each valence can possibly be explored to generate white light directly with some effectively controllable means. This approach with mixed-valence europium for white light, however, has not been fully carried out yet.

*To whom correspondence should be addressed. E-mail: dajian@tjut.edu.cn. Tel: +86 22 6021 5386. Fax:+86 22 6021 5553.

(1) Pimputkar, S.; Speck, J. S.; DenBaars, S. P.; Nakamura, S. *Nat. Photonics* **2009**, *3*, 179–181.
(2) Tonzani, S. *Nature* **2009**, *459*, 312–314.
(3) Feldmann, C.; Justel, T.; Ronda, C. R.; Schimdt, P. J. *Adv. Funct. Mater.* **2003**, *13*, 511–516.
(4) Kim, C. H.; Kwon, I. E.; Park, C. H.; Hwang, Y. J.; Bae, H. S.; Yu, B. Y.; Pyun, C. H. *J. Alloys Compd.* **2000**, *311*, 33–39.
(5) Summers, C. J.; Wagner, B. K.; Menkara, H. *3rd Int. Conf. Solid State Lighting* **2004**, *5187*, 123–132.
(6) Schubert, E. F.; Kim, J. K. *Science* **2005**, *308*, 1274–1278.
(7) Bowers, M. J.; McBride, J. R.; Garrett, M. D.; Sammons, J. A.; Dukes, A. D.; Schreuder, M. A.; Watt, T. L.; Lupini, A. R.; Pennycook, S. J.; Rosenthal, S. J. *J. Am. Chem. Soc.* **2009**, *131*, 5730.
(8) Cheng, G.; Mazzeo, M.; Rizzo, A.; Li, Y. Q.; Duan, Y.; Gigli, G. *Appl. Phys. Lett.* **2009**, *94*, 243506.
(9) Sapra, S.; Mayilo, S.; Klar, T. A.; Rogach, A. L.; Feldmann, J. *Adv. Mater.* **2007**, *19*, 569.
(10) Park, S.; Kwon, J. E.; Kim, S. H.; Seo, J.; Chung, K.; Park, S. Y.; Jang, D. J.; Medina, B. M.; Gierschner, J.; Park, S. Y. *J. Am. Chem. Soc.* **2009**, *131*, 14043–14049.
(11) Liu, J.; Zhou, Q. G.; Cheng, Y. X.; Geng, Y. H.; Wang, L. X.; Ma, D. G.; Jing, X. B.; Wang, F. S. *Adv. Mater.* **2005**, *17*, 2974.
(12) Luo, J.; Li, X. Z.; Hou, Q.; Peng, J. B.; Yang, W.; Cao, Y. *Adv. Mater.* **2007**, *19*, 1113–1117.
(13) Wang, M. S.; Guo, S. P.; Li, Y.; Cai, L. Z.; Zou, J. P.; Xu, G.; Zhou, W. W.; Zheng, F. K.; Guo, G. C. *J. Am. Chem. Soc.* **2009**, *131*, 13572.
(14) He, G. J.; Guo, D.; He, C.; Zhang, X. L.; Zhao, X. W.; Duan, C. Y. *Angew. Chem., Int. Ed.* **2009**, *48*, 6132–6135.
(15) Liao, Y. C.; Lin, C. H.; Wang, S. L. *J. Am. Chem. Soc.* **2005**, *127*, 9986–9987.
(16) Ki, W.; Li, J. *J. Am. Chem. Soc.* **2008**, *130*, 8114.
(17) Won, Y. H.; Jang, H. S.; Im, W. B.; Jeon, D. Y.; Lee, J. S. *Appl. Phys. Lett.* **2006**, *88*, 101903.
(18) Chang, C. K.; Chen, T. M. *Appl. Phys. Lett.* **2007**, *91*, 081902.
(19) Sun, X. Y. Y.; Zhang, J. H.; Zhang, X.; Lu, S. Z.; Wang, X. J. *J. Lumin.* **2007**, *122*, 955–957.
(20) Kwon, K. H.; Im, W. B.; Jang, H. S.; Yoo, H. S.; Jeon, H. S. *Inorg. Chem.* **2009**, *48*, 11525–11532.
(21) Su, Q.; Liang, H. B.; Hu, T. D.; Tao, Y.; Liu, T. *J. Alloys Compd.* **2002**, *344*, 132.
(22) Dorenbos, P. *Chem. Mater.* **2005**, *17*, 6452.
(23) Zeuner, M.; Pagano, S.; Matthes, P.; Bichler, D.; Johrendt, D.; Harmening, T.; Pottgen, R.; Schnick, W. *J. Am. Chem. Soc.* **2009**, *131*, 11242.

Published on Web 05/14/2010

We have previously proposed such a strategy that perovskite-type $LaAlO_3$ doped with coexisting valence-varied europium, in principle, achieved single-component full-color emission peaked at 450, 515, 592, and 618 nm, concurrently, and have identified that the 515-nm-peaked green emission line is assigned to the $^5D_2-^7F_3$ transition of Eu^{3+} and can be possibly enhanced through energy transfer between Eu^{2+} and the $^5D_2$ level of Eu^{3+}.[24] This valence-varied Eu-ion-doped $LaAlO_{3-\delta}$ phosphor, however, showed a dissatisfactory color rendering index (CRI) value because of the lower luminescence efficiency of 515-nm-peaked green emission. Generally, white light with CRI values as high as or greater than 80 is greatly required for indoor lighting use.[1,6] In order to efficiently tune the green emission to achieve direct white-light emission with desired CRI and correlated color temperature (CCT) values, efforts have been made in this work to detail the adjustment strategy of energy transfer for green emission between Eu^{2+} and the $^5D_2$ level of Eu^{3+} and that between Eu^{2+} and Mn^{2+} in the formula $La_{0.99-x}Sr_xAlO_{3-\delta}$:$Eu_{0.01}$ and $La_{0.994}Al_{1-x}O_{3-\delta}$:$Eu_{0.006}$, Mn_x, and $Li_{0.012}$, respectively, closely associated with the crystal structure of hosts upon substitution with Sr or Mn ions. The results have demonstrated that pure white light with high CRI and desired CCT values was successfully obtained through enhancement of the green emission, resulting from the tuning of energy transfer between Eu^{2+} and Eu^{3+}/Mn.

Experimental Section

A high-temperature solid-state synthesis procedure was employed to synthesize Sr-containing $La_{0.99-x}Sr_xAlO_{3-\delta}$:$Eu_{0.01}$ and Mn-containing $La_{0.994}Al_{1-x}O_{3-\delta}$:$Eu_{0.006}$, Mn_x, and $Li_{0.012}$ phosphors. Stoichiometric amounts of starting materials La_2O_3 (99.99%), Al_2O_3 (99.99%), Eu_2O_3 (99.99%), $SrCO_3$ (analytical reagant), and $MnCO_3$ (analytical reagant) with the desired chemical formula and doped concentration were mixed together with small amount of ethanol (analytical reagant). The slurry of starting materials was dispersed with an ultrasonator for 0.5 h and then dried at 80 °C for 12 h. Then the powders were fired at 1400 °C in a horizontal tube furnace for 4 h under a reductive atmosphere of 8 vol % H_2/92 vol % N_2 mixture.

The phases of the as-prepared phosphor samples were identified by powder X-ray diffraction (XRD) analysis (Rigaku D/max-2500/pc, $\lambda_{Cu\ K\alpha}$ = 1.54062 nm, Japan). Photoluminescence (PL) and PL of excitation (PLE) spectra of samples were recorded on a fluorescence spectrometer equipped with a xenon ligtht source (Hitachi F-4500, Japan). The slits for both excitation and emission were set as 0.25 nm, and the scan speed was fixed at 240 nm/min. The Commission International de I'Eclairage (CIE) colorimetric parameters were measured on a PMS-50 Plus UV−vis−near-IR spectrophotocolorimeter (Everine, China) system with phosphor excitation equipment. The decay time profiles and quantum yields were measured on a fluorescence spectrophotometer (Jobin Yvon FL3-221-TCSPC, U.K.) with a 450-W xenon lamp, a 340-nm Nano-LED, and an integrating sphere. The diffuse-reflectance spectra (DFS) were recorded by a TU-1901 UV−visible spectrometer (Beijing Purkinjie General, China) with a 60-mm-diameter integrating sphere (IS19-1), in which $BaSO_4$ was used as the standard reference. All of these measurements were carried out at room temperature.

Results and Discussion

Sr-Adjusted Transfer of Energy. Figure 1a shows the photoluminescence (PL) spectra for $La_{0.99-x}Sr_xAlO_{3-\delta}$:$Eu_{0.01}$ phosphor samples. In the absence of Sr substitution, the emissions peaked at 515, 537, 557, 593, and 618 nm in sharp lines are assigned to transition emissions of $^5D_2-^7F_3$, $^5D_1-^7F_1$, $^5D_1-^7F_2$, $^5D_0-^7F_1$, and $^5D_0-^7F_2$ for Eu^{3+}, respectively, while a 450-nm-peaked broad band is ascribed to a typical d−f transition emission for Eu^{2+}. Also, as the amount of Sr dopant increases, it is found that the intensity of the green emission increases but that of the blue emission decreases, implying that a transfer of energy between Eu^{2+} and the $^5D_2$ level of Eu^{3+} has effected that alternative change of the intensity because of the partial substitution of Sr for La. Accordingly, an evolutionary route of CIE chromaticity coordinates is traced to improve the quality of white-light emission, as shown in Figure 1b; i.e., the chromaticity coordinates have been tuned from the lower region of the blackbody locus to the upper one, indicating that, with an increase of Sr addition, the green-light component predominantly peaked at 515 nm has been added to the color mix for white light. Figure 1c shows photographs of visible samples to record this evolution of light-emitting color, together with the values of CRI and CCT in Table 1, upon excitation at 320 nm.

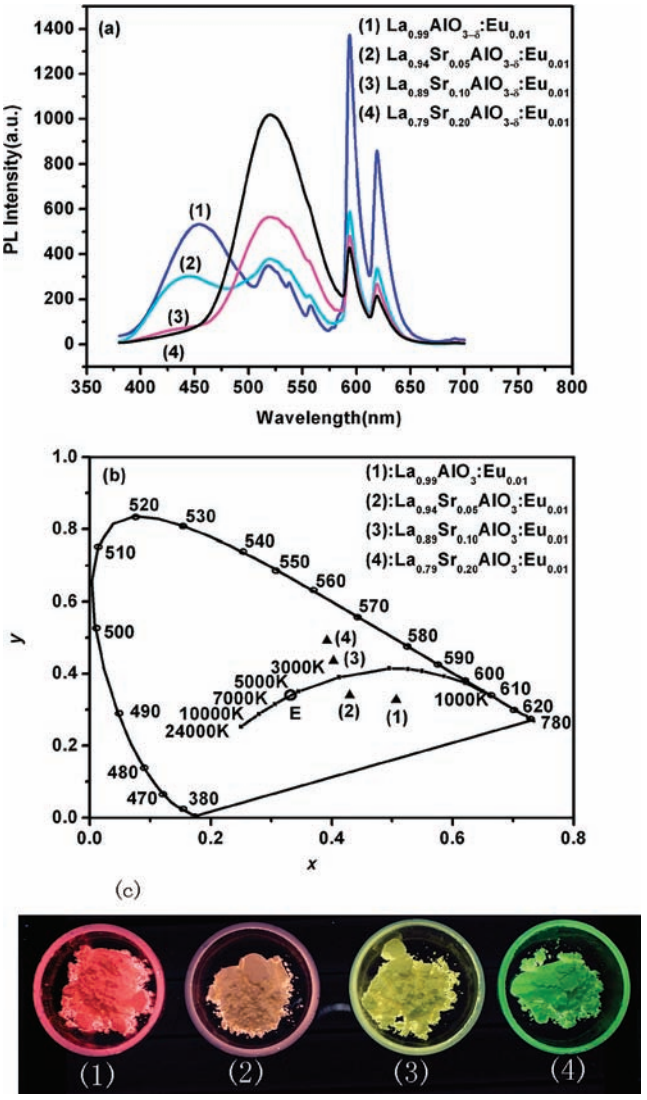

Figure 1. (a) PL spectra; (b) CIE chromaticity coordinates; (c) photographs of $La_{0.99-x}Sr_xAlO_{3-\delta}$:$Eu_{0.01}$ (x = 0.00, 0.05, 0.10, 0.20) phosphors under 320-nm excitation.

(24) Mao, Z. Y.; Wang, D. J.; Lu, Q. F.; Yu, W. H.; Yuan, Z. H. *Chem. Commun.* **2009**, 346.

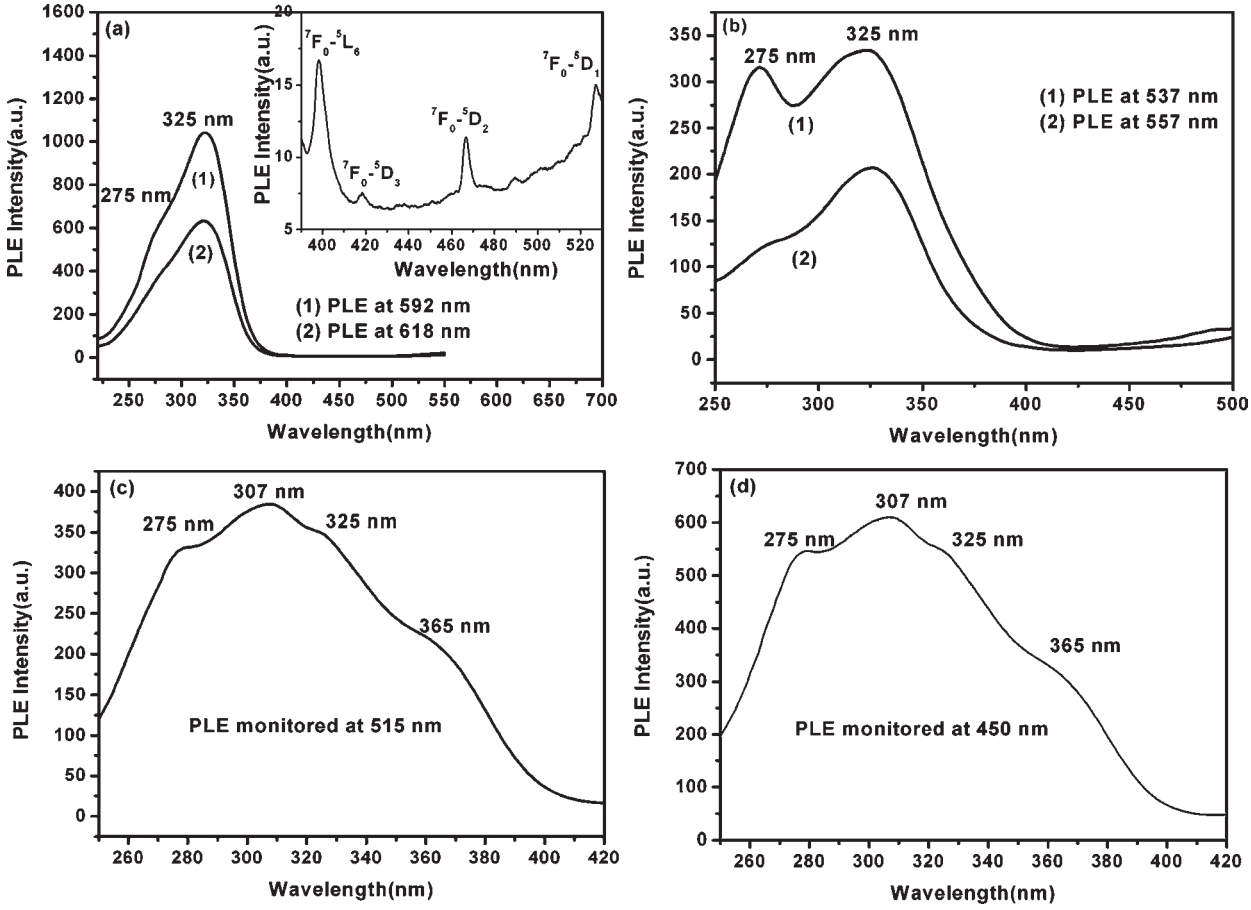

Figure 2. PLE spectra of $La_{0.99}AlO_3$:$Eu_{0.01}$ phosphors monitored at (a) 618 and 592 nm, (b) 557 and 537 nm, (c) 515 nm, and (d) 450 nm.

Table 1. CRI and CCT Values of $La_{0.99-x}AlO_{3-\delta}$:$Eu_{0.01}$ Samples

sample	CRI	CCT [K]
$La_{0.99}AlO_{3-\delta}$:$Eu_{0.01}$	48	1618
$La_{0.94}Sr_{0.05}AlO_{3-\delta}$:$Eu_{0.01}$	71	2535
$La_{0.89}Sr_{0.10}AlO_{3-\delta}$:$Eu_{0.01}$	87	3140
$La_{0.79}Sr_{0.20}AlO_{3-\delta}$:$Eu_{0.01}$	72	3400

Thus, the promised CRI values of light in varied visible colors can be tuned effectively by just controlling the amount of Sr doped properly. Furthermore, with the aid of a Li ion as a charge compensator, enhancement of the blue-light emission can be achieved.[24] Thus, white light can also be tuned through the coaddition of Sr and Li ions, based on the adjustment of the structural chemistry of the host and transfer of energy and charge compensation mechanism involved, respectively.

In the absence of Sr substitution, Figure 2 demonstrates the PLE spectra of the $La_{0.99}AlO_{3-\delta}$:$Eu_{0.01}$ sample. In Figure 2a, as monitored at 592 nm ($^5D_0-^7F_1$) and 618 nm ($^5D_0-^7F_2$), respectively, two predominant broad excitation bands are found to be located at 275 and 325 nm for the host lattice (HL) excitation and the charge-transfer state (CTS) excitation, respectively, coexisting with several sharp-line peaks located at 397, 419, 466, and 527 nm for $^7F_0-^5L_6$, $^7F_0-^5D_3$, $^7F_0-^5D_2$, and $^7F_0-^5D_1$ transitions of Eu^{3+}, respectively. Specifically, the HL excitation corresponds to the transition of valence to the conduction band of the HL and exhibits a red-shift phenomenon, as compared to single-crystal $LaAlO_3$ (~250 nm) because of the defects of the polycrystal in the powder sample, while the CTS excitation for Eu^{3+} exhibits in a broad band, generally located at around 250−400 nm. For $LaAlO_3$, this CTS excitation energy is around 4.00 eV, i.e., 320 nm,[25] which agrees well with what we have observed. It is observed that the HL and CTS excitation bands on PLE spectra reveal that energy transfer occurs between HL/CTS and $^5D_0$ and plays a key role for $^5D_0-^7F_{1,2}$ transition emissions. A similar conclusion can also be drawn for $^5D_1-^7F_{1,2}$ transition emissions by correlating the energy relationship from HL and CTS, as shown in Figure 2b, which shows PLE spectra monitored at 537 nm ($^5D_1-^7F_1$) and 557 nm ($^5D_1-^7F_2$), respectively. The PLE spectrum monitored at 450 nm (5d−4f transition emission of Eu^{2+}) is represented by Figure 2d. Except the excitation bands of HL and CTS, two other excitation bands are detected as located at 307 and 365 nm for two new bands of the $^8S_{7/2}$-5d(e_g) and $^8S_{7/2}$-5d(t_{2g}) transitions of Eu^{2+}, respectively. The presence of HL and CTS excitation bands on the PLE spectrum hints that the energy of incident photons can also be transferred from HL/CTS to Eu^{2+}. An astonishing resemblance for both the PLE spectrum monitored at 515 nm ($^5D_2-^7F_3$) and that monitored at 450 nm in parts c and d of Figure 2 reveals that an effective transfer of energy from Eu^{2+} to the $^5D_2$ state of Eu^{3+} occurs. Moreover, the HL and CTS excitation bands play a similar role for $^5D_2$ emissions of Eu^{3+}; those emissions do not originate from HL and CTS directly but from Eu^{2+} indirectly.

(25) Dorenbos, P. *J. Lumin.* **2005**, *111*, 89.

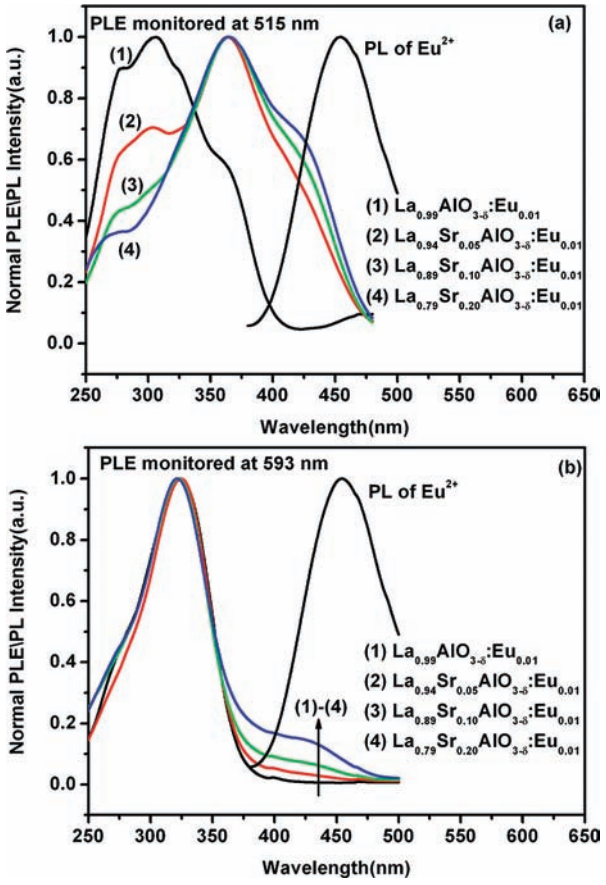

Figure 3. Normalized PLE spectra monitored at (a) 515 nm and (b) 593 nm for $La_{0.99-x}Sr_xAlO_{3-\delta}:Eu_{0.01}$ samples and normalized PL spectra of Eu^{2+} for $La_{0.99}AlO_{3-\delta}:Eu_{0.01}$ samples.

It is worth noting that the excitation bands of the f−d transition for Eu^{2+} can be identified on the PLE spectrum monitored at 515 nm but not at 537, 557, 592, and 618 nm. This phenomenon implies that the transfer of energy occurs only between the energy levels of Eu^{2+} and $^5D_2$ of Eu^{3+} but not between Eu^{2+} and all levels of Eu^{3+} in the Sr-undoped sample.

We further investigated the influence of Sr ions on energy transfer for $La_{0.99-x}Sr_xAlO_{3-\delta}:Eu_{0.01}$ samples. Figure 3 represents the normalized PLE spectra for $La_{0.99-x}Sr_x$-$AlO_{3-\delta}:Eu_{0.01}$ samples and the normalized PL spectrum of Eu^{2+} for the Sr-undoped sample. For PLE spectra monitored at 515 nm for Sr-doped samples in Figure 3a, a red shift occurs as the amount of Sr-doped sample increases. Also, three excitation bands located at 275, 365, and 425 nm are assigned to the excitation band of HL, $^8S_{7/2}$-5d(e_g) and $^8S_{7/2}$-5d($t_{2\ g}$) for Eu^{2+}, respectively. The absence of a CTS excitation band on the PLE spectrum for Sr-doped samples implies that the transfer of energy has been suppressed between CTS and Eu^{2+}. The red-shift phenomenon of the $^8S_{7/2}$-5d excitation band of Eu^{2+} is ascribed to the change of the crystal field as Sr ions are embedded in the HL. With an increase of the Sr-doped content, enlargement of the overlapping between PLE of 515 nm and PL of Eu^{2+} indicates that the energy transfer ratio between Eu^{2+} and the $^5D_2$ level of Eu^{3+} is enhanced, as shown in Figure 3a. Figure 3b shows the normalized PLE spectra monitored at 592 nm for $La_{0.99-x}Sr_xAlO_{3-\delta}:Eu_{0.01}$ samples and the normalized PL of Eu^{2+} for Sr-undoped samples. Thus, we have observed

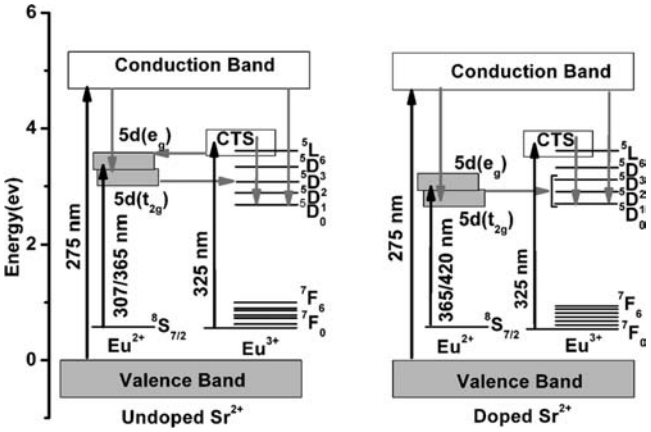

Figure 4. Energy level schemes for Sr-undoped and Sr-doped samples. Black arrow represents absorption/excitation courses, while gray arrows represent courses of energy transfer.

the shape of the $^8S_{7/2}$-5d excitation band and its enhancement with an increase of the Sr-doped concentration and enlargement of the overlapping between PLE and PL of Eu^{2+} to reveal an intensification of energy transfer between Eu^{2+} and the $^5D_0$ level of Eu^{3+}.

Enhancement of the energy transfer can be ascribed to the occurrence of oxygen vacancies because nonequivalent substitution of La^{3+} by Eu^{2+}/Sr^{2+} exists in the host. As shown in Figure 4, in the absence of Sr dopant, Eu^{2+} has a higher coordination number than that of the Sr-doped sample, leading to the formation of a centroid for the 5d state at a higher level, which shows a slight overlapping with the $^5D_2$ level and nonoverlapping with $^5D_{0,1}$ levels. The centroid of the 5d state is lowered with an increase of the Sr content because of its location at a less-coordinated site of Eu^{2+} because oxygen vacancies exist for nonequivalent substitution. As a result, the degree of overlapping and efficiency of the energy transfer between the 5d state of Eu^{2+} and the $^5D_{2,1,0}$ level of Eu^{3+} has been enhanced because of a red shift of the centroid for 5d electrons.

Mn-Adjusted Transfer of Energy. As a promising sensitizer for Mn^{2+} ions, Eu^{2+} has long been employed as an efficient sensitizer in many Mn^{2+}-doped phosphors. Figure 5a shows the PL spectra for $La_{0.994}Al_{1-x}O_{3-\delta}:Eu_{0.006}$, Mn_x, and $Li_{0.012}$ phosphor samples, in which the Li ion acts as a charge compensator. In this case, the Mn^{2+} ion emits green light located at 515 nm and superposes with the transition emission $^5D_2-{}^7F_3$ of Eu^{3+}. From Figure 5a, the intensity of the green emission band increases at the beginning and reaches a maximum as the Mn ion concentration reaches a value of 0.004 mol and then declines, indicating that a concentration quenching effect occurs, whereas the blue emission band decreases with an increase of the Mn-doped content, which can be ascribed to the energy transfer between Eu^{2+} and Mn^{2+} ions. Accordingly, Figure 5b shows the CIE chromaticity coordinates of $La_{0.994}Al_{1-x}O_{3-\delta}:Eu_{0.006}$, Mn_x, and $Li_{0.012}$ phosphors. Photographs and the CRI and CCT values of the samples upon excitation at 320 nm are demonstrated in Figure 5c and Table 2, respectively. It could be confirmed that the CIE chromaticity coordinates are tunable through adjustment of the content of the Mn-doped sample, and pure white light with a desired CRI can be achieved as the doped content is controlled to 0.002 mol.

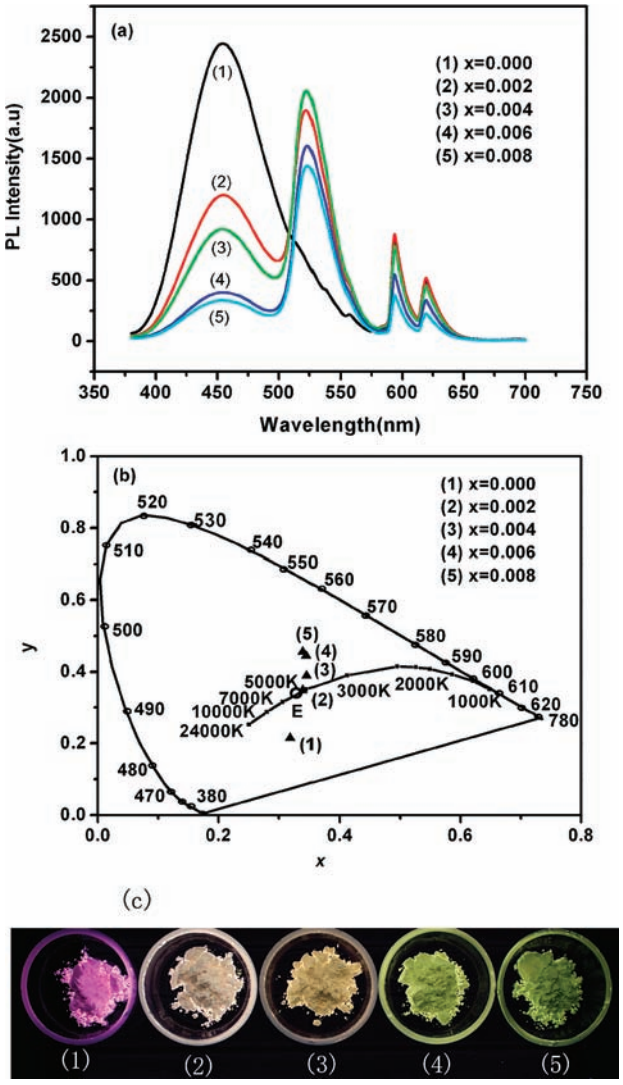

Figure 5. (a) PL spectra, (b) CIE chromaticity coordinates, (c) photographs of $La_{0.994}Al_{1-x}O_{3-\delta}$:$Eu_{0.006}$, Mn_x, and $Li_{0.012}$ (x = 0.000, 0.002, 0.004, 0.006, 0.008) phosphors under 320-nm excitation.

The mechanism of resonant energy transfer from Eu^{2+} to Mn^{2+} ions can be confirmed from Figure 5a, the same as that confirmed elsewhere.[26−28] Also, PLE spectra monitored at 453 and 515 nm show the same shape for $La_{0.994}Al_{1-x}O_{3-\delta}$:$Eu_{0.006}$, Mn_x, and $Li_{0.012}$ phosphors, indicating that green emission (including the $^5D_2-{}^7F_3$ transition of Eu^{3+} and the $^4T_1-{}^6A_1$ transition of Mn^{2+}) originates from energy transfer from Eu^{2+}, as shown in Figure 6a. For the exchange interaction of resonant energy transfer, the critical distance R_0 should be less than 0.3−0.4 nm between donors (Eu^{2+}) and acceptors (Mn^{2+}).[29] In our case, the critical concentration for Mn^{2+}, C_0, was determined to be around 0.002 mol; the primitive cell V_0 was calculated as 0.33 nm^3 with the crystal data;[30] thus, we calculated the critical distance value,

Table 2. CRI and CCT Values of $La_{0.994}Al_{1-x}O_{3-\delta}$:$Eu_{0.006}$, Mn_x, and $Li_{0.012}$ Samples

sample	CRI	CCT [K]
$La_{0.994}AlO_{3-\delta}$:$Eu_{0.006}$ and $Li_{0.012}$	30	10077
$La_{0.994}Al_{0.998}O_{3-\delta}$:$Eu_{0.006}$, $Mn_{0.002}$, and $Li_{0.012}$	80	5220
$La_{0.994}Al_{0.996}O_{3-\delta}$:$Eu_{0.006}$, $Mn_{0.004}$, and $Li_{0.012}$	85	5091
$La_{0.994}Al_{0.994}O_{3-\delta}$:$Eu_{0.006}$, $Mn_{0.006}$, and $Li_{0.012}$	86	5206
$La_{0.994}Al_{0.992}O_{3-\delta}$:$Eu_{0.006}$, $Mn_{0.008}$, and $Li_{0.012}$	86	5356

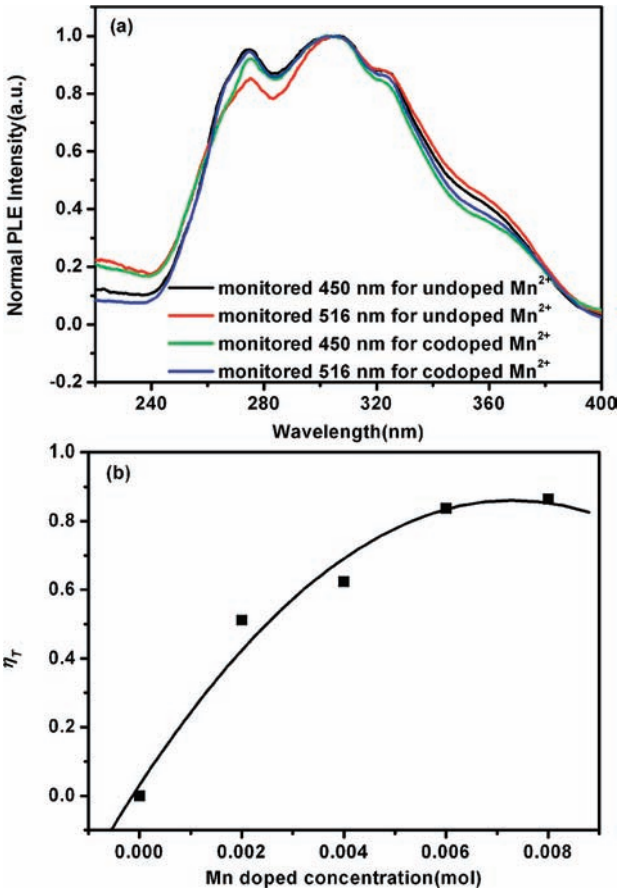

Figure 6. (a) PLE spectra monitored at 450 and 516 nm for undoped and codoped Mn $La_{0.994}AlO_{3-\delta}$:$Eu_{0.006}$ and $Li_{0.012}$ phosphors. (b) Dependence of the energy-transfer efficiency on the Mn^{2+}-doped content.

in terms of an available formula, as 3.39 nm, which is greater than 0.3−0.4 nm.[31,32] Thus, the type of resonant energy transfer between Eu^{2+} and Mn^{2+} in $La_{0.994}Al_{1-x}O_{3-\delta}$:$Eu_{0.006}$, Mn_x, and $Li_{0.012}$ phosphors is confirmed to be classified as multipolar interaction. On the basis of Dexter's energy-transfer formula of multipolar interaction and Reisfeld's approximation,[33−35] the dipole−dipole mechanism can also be confirmed for this Eu- and Mn-codoped phosphor. As shown in Figure 6b, the observed energy-transfer efficiency (η_T) from Eu^{2+} to Mn^{2+} has been demonstrated by many authors[36] and here is calculated as a function of the Mn-doped concentration in $La_{0.994}Al_{1-x}O_{3-\delta}$:$Eu_{0.006}$,

(26) Shim, M. D.; Sibley, W. A. *Phys. Rev. B: Condens. Matter* **1984**, *29*, 3834.
(27) Chang, C. K.; Chen, T. M. *Appl. Phys. Lett.* **2007**, *90*, 161901.
(28) Guo, C. F.; Luan, L.; Ding, X.; Huang, D. X. *Appl. Phys. A: Mater. Sci. Process* **2008**, *91*, 327.
(29) Antipenk, B. M.; Bataev, I. M.; Ermolaev, V. L.; Lyubimov, E. I.; Privalov, T. A. *Opt. Spectrosc.* **1970**, *29*, 177.
(30) Lehnert, H.; Boysen, H.; Dreier, P.; Yu, Y. *Z. Kristallogr.* **2000**, *215*, 145.
(31) Van Uitert, L. G. *J. Lumin.* **1974**, *4*, 1.
(32) Jiao, H.; Liao, F. H.; Tian, S. J.; Jing, X. P. *J. Electrochem. Soc.* **2003**, *150*, H220.
(33) Dexter, D. L. *J. Chem. Phys. A* **1953**, *21*, 836.
(34) Dexter, D. L. *J. Chem. Phys. B* **1954**, *22*, 1063.
(35) Reisfeld, R.; Greenberg, E.; Velapoldi, R. *J. Chem. Phys.* **1972**, *56*, 1698.
(36) Paulose, P.; Jose, L. G.; Thomas, V.; Unnikrishnan, N. V.; Warrier, K. R. *J. Phys. Chem. Solids* **2003**, *64*, 841.

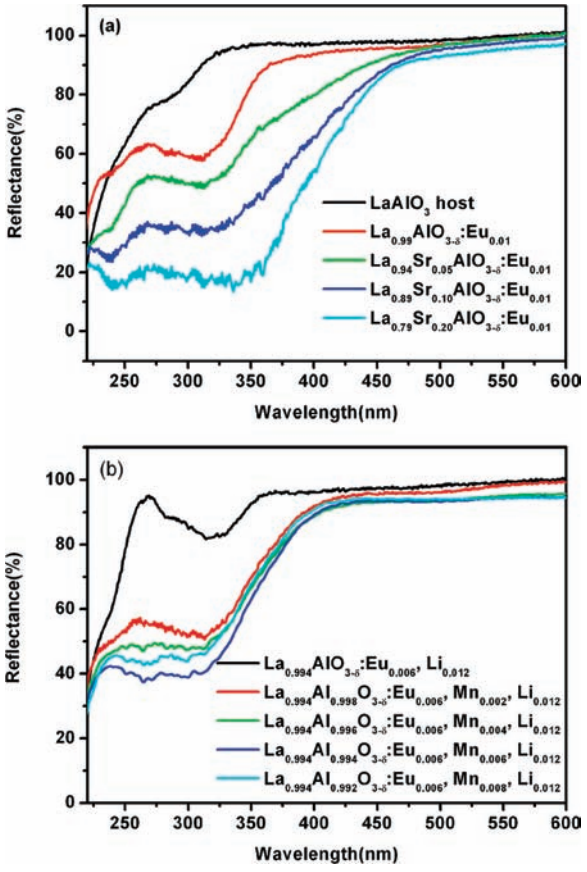

Figure 7. DFS of (a) the $LaAlO_3$ host and $La_{0.99-x}Sr_xAlO_{3-\delta}$:$Eu_{0.01}$ and (b) $La_{0.994}Al_{1-x}O_{3-\delta}$:$Eu_{0.006}$, Mn_x, and $Li_{0.012}$ samples.

Mn_x, and $Li_{0.012}$ phosphors. η_T is found to increase with an increase of the Mn content.

Figure 7 shows the DFS of the $LaAlO_3$ host, $La_{0.99-x}Sr_xAlO_{3-\delta}$:$Eu_{0.01}$, and $La_{0.994}Al_{1-x}O_{3-\delta}$:$Eu_{0.006}$, Mn_x, and $Li_{0.012}$ samples. An absorption band peaked at around 270 nm exists, corresponding to the valence-to-conduction band transitions of the $LaAlO_3$ HL. In the Eu-doped $La_{0.99}AlO_{3-\delta}$:$Eu_{0.01}$ and $La_{0.994}AlO_{3-\delta}$:$Eu_{0.006}$, and $Li_{0.012}$ samples, two absorption bands are in the wavelength range from 325 to 365 nm, which can be attributed to the CTS absorption of Eu^{3+} and the transition absorption from the ground-state $4f^7$ of Eu^{2+} to its excited state $4f^65d$, respectively. With an increase of the Sr-ion-doped content, an obvious red shift is observed on the DFS for the transition absorption band of Eu^{2+} for the Sr-ion-doped samples, as shown in Figure 7a. Also, the absorption intensity is enhanced with an increase of the doped content of Sr or Mn ions. These results from the DFS agree well with those from the PLE spectra mentioned above. The luminescence quantum efficiency of the as-prepared sample was measured at around 10% at room temperature.

Conclusions

The combination of featured transition emissions from coexisting Eu^{2+} and Eu^{3+} lanthanum aluminate happen to mix white-light color directly, in which the intensity change of 515-nm-peaked green-light emission for the $^5D_2-^7F_3$ transition of Eu^{3+} is closely associated with that of the host structure, energy transfer, and transition emission as well. Further investigations on the valence stability of europium or photostability for lanthanum aluminate in service are presently in progress. A trade-off between the color rendering and luminous efficacy of white light should also be taken into account further. The direct white-light strategy of the coexisting valence adjustment exemplified by this valence-varied europium−lanthanide aluminate could provide an option to develop some new materials in the white-light technology for lighting and display.

Acknowledgment. The authors thank The National Natural Science Foundation of China through Grant 50872091 and Key Discipline of Physical Chemistry (Tianjin, China) through Grants 06YFJMJC02300 and 2006ZD30 for financial support.

Supporting Information Available: Measurements of CIE colorimetric parameters, the origin of 515 nm green-light emission, structure and vacancy analysis, relationship between covalence and the crystal structure, and EDS elemental analysis. This material is available free of charge via the Internet at http://pubs.acs.org.